

INFLUENCE OF POST DEPOSITION THERMAL ANNEALING ON THE OPTICAL CHARACTERISTICS OF HAFNIA NANOFILMS

A. JAVED^a, M. F. WASIQ^b, A. M. RANA^a, M. Y. NADEEM^b, N. A. NIAZ^{a*},
M. E. MAZHAR^a, M. N. USMANI^a, R. CIANCIO^c, P. ORGIANI^d,

^a*Department of Physics, Bahauddin Zakariya University, Multan 60800, Pakistan.*

^b*Department of Physics, Quaid-i-Azam University, Islamabad, Pakistan.*

^c*CNR IOM TASC, Area Science Park Basovizza, I-34149 Trieste, Italy.*

^d*CNR-SPIN and Department of Industrial Engineering, University of Salerno, I-84084 Fisciano (SA), Italy*

Hafnia nanofilms of 60 nm thickness were deposited on Corning glass substrates at different substrate temperatures (from 25 to 120 °C) by applying electron-beam evaporation technique. After deposition, all the nanofilms were thermally annealed at temperatures between 300 to 500 °C for about half an hour in vacuum conditions. All the post thermally annealed nanofilms were characterized through x-ray diffraction and spectrophotometry. Structural characterizations showed that all the as-deposited hafnia nanofilms and the films annealed up to a temperature of 400 °C were amorphous in nature and the films annealed at 450 °C and 500 °C were transformed to polycrystalline phase possessing monoclinic structure. Hafnia nanofilms possessing different morphologies and crystallite sizes demonstrate variations in the optical properties including refractive index (1.88–2.94), optical band gap energy (3.29–3.85 eV), extinction coefficient (0.023–0.063) etc. Almost all the optical parameters portray oscillatory trend as a function of substrate temperature, which may be attributed to the removal of any residual stresses as well as to the transformation of amorphous phase to polycrystalline one and crystallite growth at high annealing temperatures. In addition, both un-annealed and annealed hafnia nanofilms depicted high reflectance (50–70%) in the visible region. Further improvement in reflectance can be made by inserting a metallic layer to form the oxide–metal–oxide stack morphology, which might have possible applications as heat mirrors. On the basis of above mentioned facts, a noteworthy conclusion is that the substrate temperature and post thermal annealing possesses greater tendency of changing the structural and optical properties of hafnia nanofilms.

(Received December 28, 2017; Accepted March 12, 2018)

Keywords: Post thermal annealing, Optical band gap energy, X-ray diffraction, Nanofilms.

1. Introduction

Studies of thin films have shown advancement in many new areas of research in solid-state chemistry and physics based on unique characteristics of their thickness, geometry and micro-structures. The ability of material scientists and engineering community to conceive the novel materials with extraordinary combination of optical and structural properties have changed the modern society. Thin film's application related to the optical properties include optical coatings, magnetic films for data storage, optical data storage devices etc. [1]. Innovative use of the interference processes in thin films lead to develop refined multilayered structures, which depict almost ideal reflection, polarization, antireflection, narrow and wideband reflection, as well as transmission filtering properties [2,3]. Thin film coatings are beneficial in enhancing thermal performance of window glazing giving new aspects in the artistic features of building design [3].

*Corresponding author: niazpk80@gmail.com

Hafnium oxide (HfO_2) usually exists in four different crystalline states e.g. monoclinic, tetragonal, cubic and orthorhombic possessing differing values of dielectric constants [4,5]. Among these, monoclinic phase is found stable at room temperature [6]. Hafnia films have high dielectric constant, high refractive index, large band gap energy, bulk modulus, melting point and good chemical stability which make these films suitable for optical and structural usages [7]. Mainly, being high-k material HfO_2 can be good replacement for gate dielectrics in FETs, CMOS [8] and dynamic RAMs [7]. Because of wide band gap (~ 5.5 eV) [9] it depicts transparency over widespread spectral range, which extends from UV to mid-infrared region [10]. That is why, hafnia films are used in optical coatings such as filters, beam splitters, highly reflective mirrors and anti-reflection coatings [11,12]. It is found that optical parameters show different values if films are prepared by thermal evaporation in different laboratories depending on different deposition systems. Various deposition techniques have been reported to fabricate thin films like RF-sputtering [12-14], ion beam evaporation [10,15], conventional electron beam evaporation [10,11,16,17], atomic laser deposition (ALD) [18], pulsed laser deposition (PLD) [19] and chemical vapor deposition [9]. Among these electron beam evaporation is the simplest technique which has advantages like good control on deposition rates, tremendous material consumption and contamination free as compared to other methods [20,21] such as sputtering, which transports contamination and causes high defect density in the deposited films [22–24]. Thermal annealing is known to have sufficient affinity of influencing structural, optical and electrical properties of hafnia thin films composed of nanoparticles [25]. In addition, post thermal annealing has been noted as beneficial for closely packed hafnia thin films by reducing the defects as described by Tan et al. [20]. Such hafnia films of high transparency over the entire solar spectrum may be suitable for heat mirrors applications, whose performance depends mainly on optical parameters, thickness of metal and metal oxide film [26].

In the present research work, structural and optical properties of hafnia nanofilms deposited by electron beam evaporation technique have been reported. Structural and optical characterizations of these hafnia nanofilms have been performed in the un-annealed and thermally annealed conditions using spectrophotometry and x-ray diffraction (XRD). XRD data reveals amorphous phase transformed to monoclinic structure. While spectral data shows the effects of quantum confinement on optical band gap energy tailoring in thermally annealed hafnia nanofilms. These nanofilms appear to be better reflector of radiations for possible applications as heat mirrors and transparent conducting materials.

2. Experimental work

Hafnium oxide nanofilms have been fabricated through electron beam evaporation technique in the Edward EA306A deposition unit on Corning glass substrates at five different substrate temperatures, i.e., 25, 50, 80, 100 and 120 °C. Hafnia nanofilms having thickness of ~ 60 nm have been deposited using granular hafnium oxide (99.95% pure) using graphite crucibles. The pressure of deposition chamber was kept at 5×10^{-5} Torr and monitored by Pirani and Penning gauges. The backing of vacuum chamber was done prior to deposition for at least 2 hours. The rate of deposition and thickness of nanofilms were measured by a calibrated quartz crystal monitor (Edward FTM7). However, actual thicknesses of these films were determined using spectroscopic ellipsometry. It was noted a difference between two measurements of the order of ± 2 nm. High rates of deposition were obtained due to better sticking of the evaporated material to the substrate and in good vacuum conditions. It is known that suitable choice of thin film deposition parameters needs better care because deposition technique, deposition conditions including chamber pressure, deposition time, film thickness, rate of deposition, kind of the source material and nature of substrate over which film growth starts, pose significant effects on various properties of the deposited material. That is why different factors adjusted/recorded at or during film deposition are shown in Table 1.

Table 1. Deposition parameters for hafnia nanofilms.

Sr. No.	Sample ID	Thickness (nm)	Pressure ($\times 10^{-5}$ Torr)	Temp. ($^{\circ}$ C)	Deposition Rate (nm/sec)	Deposition Time	Current (mA)
1	BB	60	5.0	RT	0.09	12:43	110
2	BE	60	5.0	50	0.21	12:01	100
3	BH	60	5.5	80	0.21	10:00	100
4	BK	60	5.0	100	0.12	14:58	100
5	BN	60	6.0	120	0.06	25:56	100

After film deposition, all the deposited films were annealed in a vacuum better than 10^{-3} Torr at temperatures in the range from 300 to 500 $^{\circ}$ C for about 30 minutes. Crystal structure of all the annealed films was studied by recording X-ray diffraction (XRD) patterns at room temperature using PANalytical Empyrean diffractometer equipped with Cu K α radiations having wavelength of 0.15406 nm in the diffraction angle (2θ) range of 10–80 $^{\circ}$. To record optical absorbance and transmittance spectra at room temperature and in the wavelength range of 250–850 nm, SHIMADZU UV-1800 UV-VIS Spectrophotometer was used.

3. Results and discussion

3.1. Structural properties

The investigation related to microstructure and related properties of HfO $_2$ nanofilms are of significant importance for the development of novel functional materials possessing unique and promising properties. Electron beam evaporated hafnia nanofilms having thickness of \sim 60 nm deposited at different substrate temperatures ranging from room temperature (25 $^{\circ}$ C) to 120 $^{\circ}$ C have been analyzed for their structural and optical behavior for their possible applications in optical industry. It is observed that these films on Corning glass slides are physically stable and show very good adhesion to their substrates. These films were investigated to study their microstructural nature on post thermal annealing at temperatures between 300 to 500 $^{\circ}$ C by recording XRD patterns as shown in Figs. 1 and 2. Fig. 1 illustrates only two broad peaks lying in the 2θ range starting from 15 to 35 $^{\circ}$ and from 40 to 70 $^{\circ}$ for a typical specimen as representative of all the as-deposited films illustrating no sharp peak which confirms the amorphous nature of these nanofilms. On post thermal annealing of these films at various intermediate temperatures for about half hour, XRD investigations were repeated and results of these diffraction studies are demonstrated in Fig. 2. These patterns illustrate that the post thermal annealing has caused some structural modifications in these films. It is noticeable that all the films annealed up to a temperature of 400 $^{\circ}$ C still depict only broad peaks leading to amorphous nature but the films annealed at 450 $^{\circ}$ C and 500 $^{\circ}$ C have changed their state from amorphous to polycrystalline one. The observed diffraction peaks have been identified with the help of ICDD card no. 06-0318. It is noted that all these peaks correspond to HfO $_2$ monoclinic structure having space group P21/c [27] and lattice parameters; $a = 5.12$ \AA , $b = 5.18$ \AA and $c = 5.25$ \AA . Furthermore, weak intensity of the diffraction peaks (as shown in Fig. 2) except main peaks and a broad reflection between 15 to 30 $^{\circ}$ might lead to the presence of some disordered phase at 450 $^{\circ}$ C. Increasing intensity of XRD reflections signifies an improvement in crystallinity of thin films. In addition, broadening of these peaks suggests the crystallites to have nanosize. Average size of the crystallites was determined using the well-known Scherer's formula [28]:

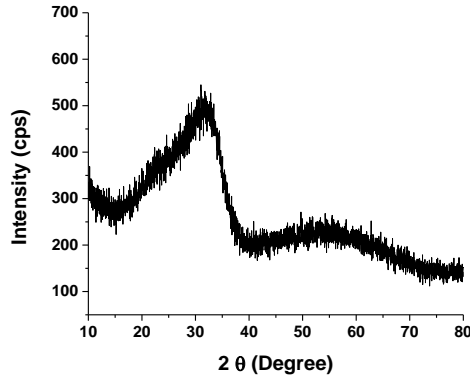


Fig. 1. X-ray diffraction pattern of a typical specimen of as-deposited HfO_2 nanofilm before thermal annealing.

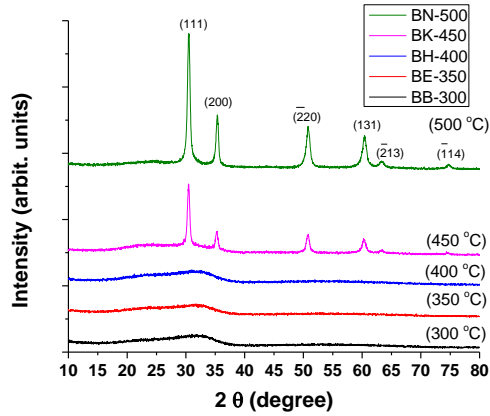


Fig. 2. X-ray diffraction spectra of thermally annealed HfO_2 nanofilms deposited at various substrate temperatures (i.e. at 25 (BB), 50 (BE), 80 (BH), 100 (BK), and 120 (BN) °C).

$$t = 0.9 \lambda / \beta \cos \theta \quad (1)$$

where λ is the wavelength of the x-rays, θ is the diffraction angle, and β is the corrected full width at half maximum (FWHM) of the diffraction peak given by [29]:

$$\beta^2 = \beta_m^2 - \beta_s^2 \quad (2)$$

where β_m is the measured FWHM, and β_s is the FWHM of a standard HfO_2 specimen with crystallite size in the range of 100 nm. The average size of hafnia crystallites as determined by applying Eq. (1) is found to increase from 14.1 nm to 15.1 nm on increasing annealing temperature from 450 to 500 °C. It means that increasing annealing temperature not only improves crystallinity but also contributes in growth of the crystallites. Such crystallization of HfO_2 films may be accountable for any variations in the optical characteristics [20,22, 23, 30, 31].

3.2. Optical Characterization

3.2.1. Optical Transmittance and Energy band gap

Optical transmittance spectra of all thin films were determined in the UV/Visible range i.e. 250–850 nm. Measured transmittance (T) variations before and after annealing at various temperatures in the range from 300 to 500 °C for half an hour of each film deposited at different substrate temperatures are shown in Fig. 3. These plots clearly show that transmittance is very strong (>70%) in the visible region, however, a sudden fall in transmittance is observed in each

film in the UV-range, i.e. 250–350 nm. It is obvious that the fundamental absorption edge exits in the UV region. Such a high level of transmittance in the visible region proposes the lack of any electronic transition from valence to conduction bands of hafnia nanofilms.

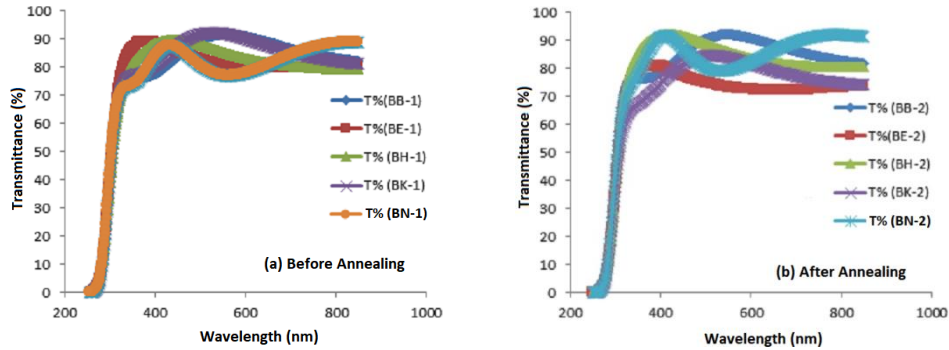


Fig. 3. Optical transmittance (T) spectra of hafnia nanofilms a) before and b) after thermal annealing at various temperatures.

Table 2. Various optical parameters obtained for hafnia nanofilms.

Sample (60 nm)	Refractive Index (at 632.8 nm)			Dielectric Constant		Extinction Coefficient		Band Gap Energy (eV)		Urbach Energy (eV)	
	n1**	n1*	n2*	ϵ_1	ϵ_2	k1	k2	E_{g1}	E_{g2}	$\Delta E1$	$\Delta E2$
BB (300 °C)	8.27	1.88	1.89	3.53	3.57	0.023	0.024	3.86	3.81	0.237	0.242
BE (350 °C)	8.87	2.46	2.94	6.05	8.64	0.047	0.063	3.76	3.70	0.246	0.254
BH (400 °C)	8.72	2.33	2.30	5.43	5.29	0.042	0.040	3.62	3.59	0.265	0.272
BK (450 °C)	8.46	1.95	2.40	3.80	5.76	0.026	0.046	3.45	3.50	0.290	0.253
BN (500 °C)	8.50	2.44	1.89	5.95	3.57	0.036	0.026	3.29	3.42	0.250	0.246

* 1 denotes values for unannealed films while 2 denotes values for annealed films in all cases.

** at wavelength of 290 nm.

The investigations of fundamental absorption is vital in providing valued information about optical band gap energy, inter-/intra-band electronic transitions etc. [32]. Optical absorption is related to transmittance through the relation: $A = \log\left(\frac{1}{T}\right)$, where A is the optical Absorbance.

Absorption coefficient (α) can be obtained through the relation: $\alpha = 2.303A/x$, where x gives the thickness of hafnia films (~60 nm). It is found that fundamental absorption edge in the absorption spectrum appears because of optically induced electronic transitions from valance to conduction bands and it demonstrates itself through a rapid fall in transmittance spectrum according to its dependence as proposed by Mott and Davis [33]. Optical changes in absorption coefficient $\alpha(\omega)$ in the region of fundamental absorption edge can be well fitted to the Tauc relation [34]:

$$\alpha \hbar \omega = B(\hbar \omega - E_g)^m \quad (3)$$

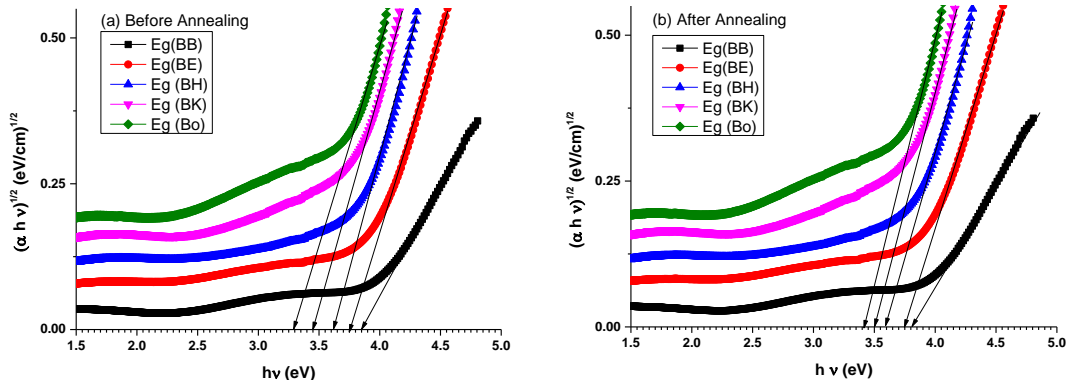


Fig. 4. The $(\alpha h\nu)^{1/2}$ vs. photon energy ($h\nu$) graphs plotted to determine energy band gap both in (a) unannealed and (b) thermally annealed HfO_2 nanofilms.

where $h\nu$ is the incident photon energy, E_g the energy band gap, B the transition characteristic parameter (independent of photon energy) and m is an index that specifies the type of transition i.e. $m = 2$ or 3 for allowed or forbidden indirect transitions, while $1/2$ or $3/2$ for allowed or forbidden direct transition respectively.

Eq. (3) requires that in the region of fundamental absorption edge, $(\alpha h\nu)^{1/m}$ should vary linearly with photon energy, $h\nu$. Therefore, on the extrapolation of linear part of such plot to $(\alpha h\nu)^{1/m} = 0$, value of E_g can be obtained for some particular transition. These plots for $m = 2$ (allowed indirect transitions) are drawn both for annealed and un-annealed HfO_2 films are shown in Fig. 4. For various substrate temperatures the band gap values thus obtained are given in Table 2. It is notable from this table that E_g values decrease with a rise of substrate temperature. However a comparison of band gap values before and after annealing hafnia films (Table 2) shows small decrease in E_g values for those films which remained amorphous after annealing but E_g values increased for those films which transformed into polycrystalline phase. Values of band gap before annealing are found to be between 3.86 eV and 3.29 eV but for annealed films these values are from 3.81 eV to 3.42 eV. This small decrease in band gap after annealing may be attributed to slight structural modifications and removal of residual stresses etc. whereas rise of E_g values can be related with transformation of microstructure from amorphous to polycrystalline one [30,35] as observed through XRD (Fig. 2). It has already been proposed that the band structure is significantly influenced by structural transformations [23]. The changes in energy band gap values on rising substrate temperature are displayed in Fig. 5. The observed variation in E_g may be associated with the readjustment of atoms and molecules to more favorable positions/stable states by post thermal annealing [36]. In addition, such changes in band gap energies with annealing/substrate temperatures may be caused by size-dependent quantum confinement effects in nanofilms [36].

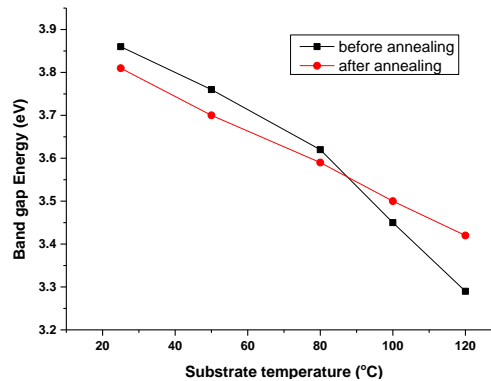


Fig. 5. Plots showing band gap energy variations with change in substrate temperature in un-annealed and thermally annealed HfO_2 nanofilms.

3.2.2. Urbach energy and extinction coefficient

The absorption coefficient $\alpha(\omega)$ in the exponential-edge region can be articulated by well-known relationship termed as Urbach formula [37,38]:

$$\alpha(\omega) = \alpha_0 \exp(\hbar\omega / \Delta E) \quad (4)$$

Where α_0 is a constant and ΔE the Urbach energy that can be described by the slope of an exponential edge portion and inverse of this slope provides width of the band tailing caused by localized states appeared due to defects/disorder associated with amorphous nature of nanofilms in the region of gap between conduction and valence bands. It was suggested that such exponential dependence of absorption coefficient on the energy of photons may appear due to random variabilities in the internal fields linked to structural disorder in many amorphous materials [39].

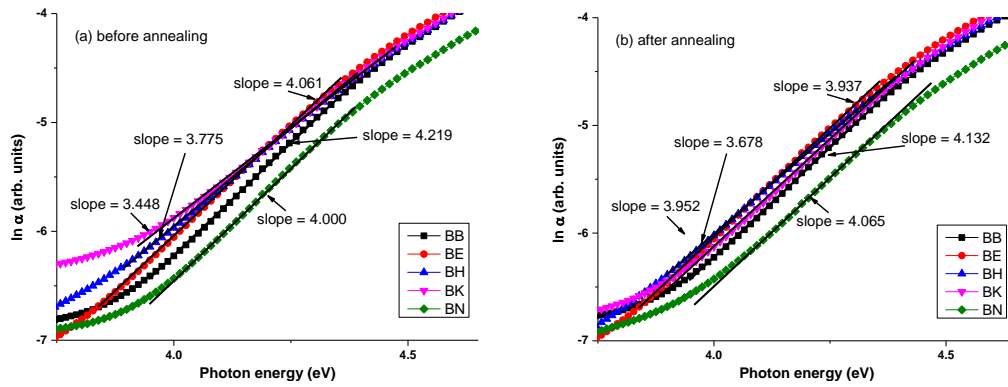


Fig. 6. Plots showing Urbach energy variations with change in photon energy in (a) unannealed and (b) thermally annealed HfO_2 nanofilms.

In addition, such exponential behavior of $\alpha(\omega)$ is induced by electronic transitions between localized states and density of localized states decreases exponentially with photon energy [40].

In order to determine the width of band tailing caused by the disordered nature of hafnia nanofilms, plots of $\ln(\alpha)$ vs. photon energy ($\hbar\omega$) are made both for un-annealed and annealed films as presented in Fig. 6. The ΔE values as determined from the slopes of these graphs are also given in Table 2. Comparing the Urbach energy ΔE values before and after annealing, it is seen that ΔE values increase because of annealing which suggests increase of band tailing width, consequently leading to decrease in band gap energy E_g . The extinction coefficient k can be related with absorption coefficient through the following equation [36]:

$$k = \alpha\lambda/4\pi \quad (5)$$

The extinction coefficient [calculated using Eq. (5)] variations as a function of wavelength λ are depicted in Fig. 7 for annealed and un-annealed hafnia nanofilms. Any rise or fall in k depends on the absorption coefficient as well as wavelength, that is why, the consequential plots look much similar to those expected for absorbance. The values of k obtained in the UV region for both annealed and un-annealed hafnia nanofilms are also tabulated in Table 2, which illustrates very low loss of energy.

3.2.3. Reflectance and Refractive index

Fig. 8 illustrates reflectance changes in un-annealed and thermally annealed hafnia nanofilms as a function of wavelength. Reflectance R is found to be much higher in the range from 50% to 70% in the visible region. Moreover, reflectance demonstrates oscillatory trend with increasing wavelength in the visible region. It is noticeable that in spite of the material, a wavelength where there is a strong absorption there will in general be a robust reflection. Similar

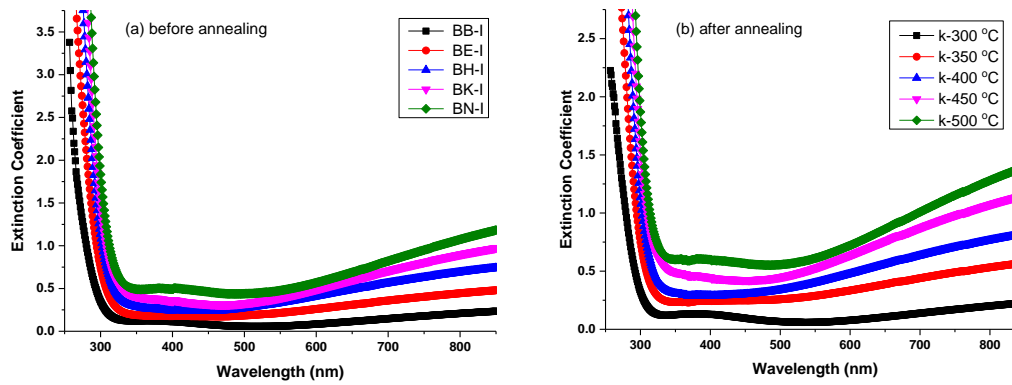


Fig. 7. Graphs of extinction coefficient k plotted against wavelength for (a) unannealed and (b) annealed hafniananofilms

type of behavior can be observed in the visible part of radiations for semiconductors depicting an interband absorption while ionic materials demonstrate such behavior in the infrared region at the ionic resonance frequencies [41]. The reflectance data is useful for finding the refractive index of a material. In the case of normal incidence, refractive index n is found to have relation with the reflectance as given below [36,42]:

$$n = \frac{1 + \sqrt{R}}{1 - \sqrt{R}} \quad (6)$$

Refractive index was calculated using Eq. (6) and is presented as plots in Fig. 9 as a function of wavelength. It is noted that n illustrates oscillatory behavior with wavelength in the visible region. Such oscillatory trend may be associated with the polarization process since n depends upon the extent of polarization. The n values obtained at $\lambda = 290$ nm before annealing these nanofilms are found to be much higher in the range of 8.27-8.87 but n values at $\lambda = 632.8$ nm are in the range of 1.88-2.46. However, at this wavelength n values for annealed hafnia nanofilms are between 1.89 and 2.94, which are slightly larger than those for un-annealed nanofilms as clear from Table 2. These variations may be associated with variations in the density of these nanofilms because of annealing which not only removed any residual stresses but also crystallized the films annealed at 450 and 500 °C. Present results are somewhat different from those of Ni et al. [21], who have suggested that refractive index of amorphous films is high in comparison with polycrystalline ones but for textured films, n is high again. It means that hafnia nanofilms with higher texture have higher values of n which is larger than its counterpart. The variations of refractive index with substrate temperature indicate almost oscillatory trend in both cases. This type of oscillatory trend of n with increasing substrate temperature could be attributed to crystallization and crystal growth as described by XRD. Wang et al. [43] have noticed that polycrystalline hafnia thin films fabricated by plasma-ion-assisted deposition have low values of refractive index as noted in the present study in the visible range. They suggested that high inhomogeneity due to high deposition rate might lead to larger plasma-ion momentum transfer per deposition atom. While e-beam deposited polycrystalline hafnia thin films depicted higher n values with high deposition rates [44]. The present results closely agree with results of Ref. [44], since better sticking and suitable evaporation rates combined with annealing produced relatively homogeneous films yielding the lowest n value 1.88 at wavelength of 632.8 nm.

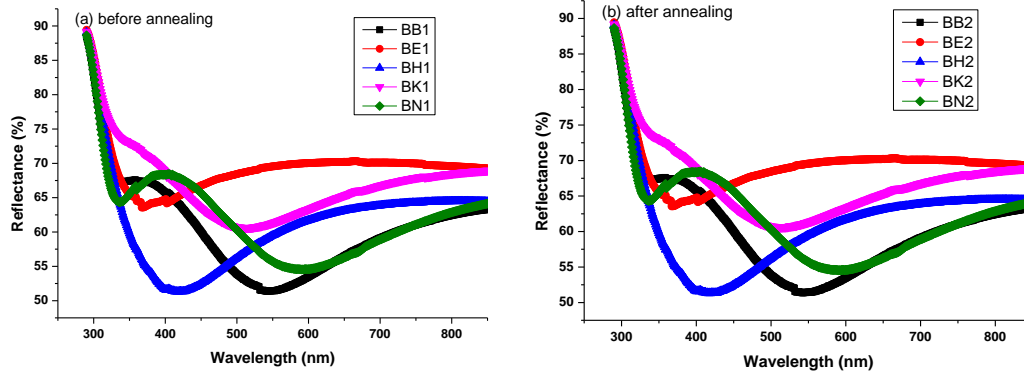


Fig. 8. Optical reflectance (R) spectra at normal incidence of light for hafnia Nanofilms; (a) before and (b) after thermal annealing.

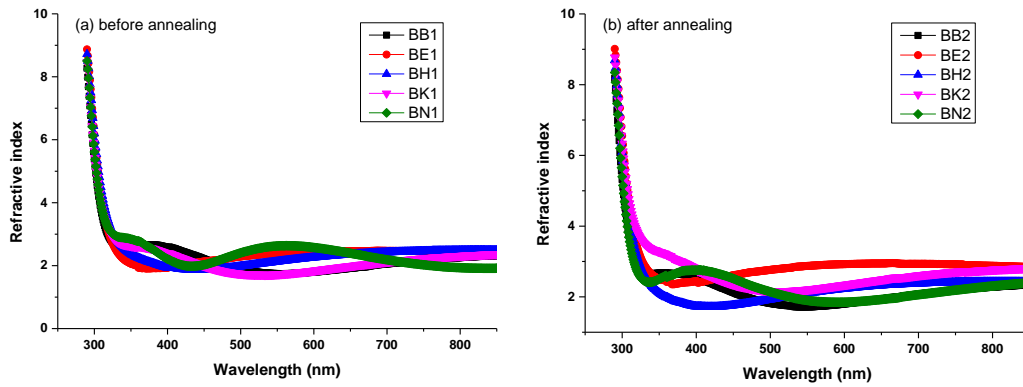


Fig. 9. Plots of refractive index n drawn against wavelength for (a) unannealed and (b) annealed hafnia nanofilms.

3.2.4. Molar Reflectivity and Relative Permittivity (Dielectric Constant)

Molar reflectivity R_m and molar volume V_m are linked with refractive index n through a relation proposed by Fanderlik [45] as follows:

$$\frac{R_m}{V_m} = \frac{n^2 - 1}{n^2 + 1} \quad (7)$$

By applying Eq. (7), molar reflectivity per unit molar volume can be calculated and the obtained values are then plotted against wavelength as demonstrated in Fig. 10. These graphs show oscillatory character of R_m/V_m in the visible region.

Dielectric constant also called relative permittivity, ϵ , of un-annealed and annealed hafnia nanofilms can be calculated using the relation: $\epsilon = n^2$, and the results are displayed in Fig. 11. It is seen that the relative permittivity changes in an oscillatory manner in the visible region. Moreover, in visible region of light ϵ possesses values in the range of 2.8 to 8.5 and from 2.8 to 10.0 for un-annealed and annealed hafnia nanofilms respectively.

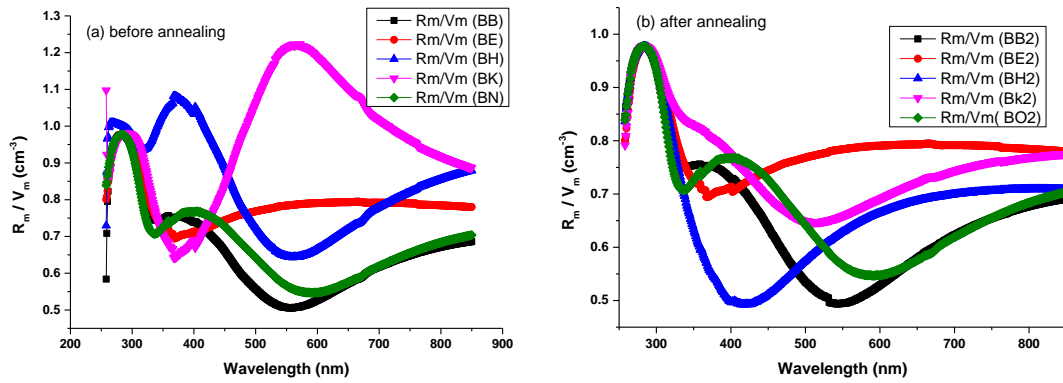


Fig. 10. Plots of molar refractivity per unit molar volume, R_m/V_m , drawn against wavelength for (a) unannealed and (b) annealed hafnia nanofilms.

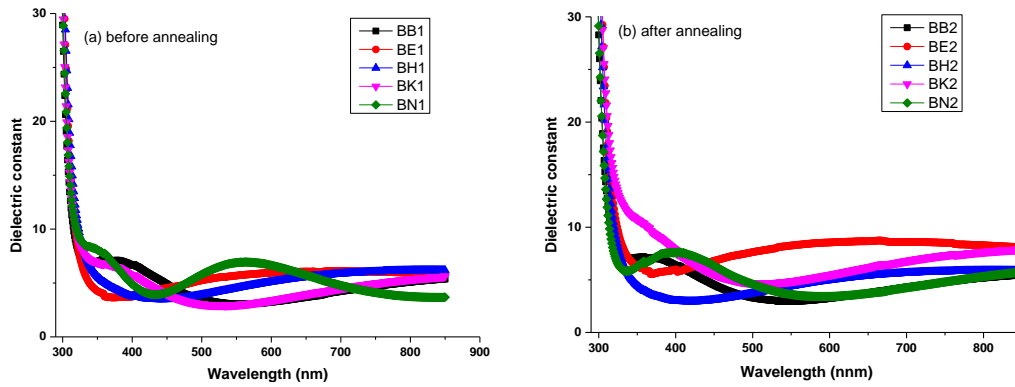


Fig. 11. Plots of dielectric constant, ϵ , vs. wavelength for (a) unannealed and (b) annealed hafnia nanofilms.

4. Conclusions

Hafnia nanofilms were fabricated at various substrate temperatures ranging from room temperature 25 °C to 120 °C and are amorphous in nature. These nanofilms were converted into polycrystalline monoclinic phase on annealing at temperatures of 450 and 500 °C for half an hour. Such thermal annealing was found to vary structural and optical properties of hafnia nanofilms. Any variation observed in film morphology and crystallite size caused by annealing was held responsible for observed changes in optical parameters. Optical parameters e.g. band gap energy, refractive index, extinction coefficient etc. of these hafnia nanofilms exhibit oscillatory trends with rising substrate temperature and thermal annealing. The studied hafnia nanofilms depict high reflectance (50–70%) in the visible region which appears to be suitable for their expected applications as a heat mirror.

Acknowledgements

Authors gratefully acknowledge the support provided by Dr. F. Chollet (Micro-Machines Centre, School of Mechanical and Aerospace Engineering, Nanyang Technological University, Singapore) during nanofilms fabrication and some characterization facilities. In addition, financial support of Higher Education Commission (HEC) Pakistan through 6 months IRSIP Scholarship Scheme is highly appreciated.

References

- [1] K. L. Chopra, "Thin Film Phenomena", McGraw-Hill, New York (1969), p. 267.
- [2] C.C. Lee, S.H. Chen, C.C. Jaing, *Appl. Opt.* **35**, 5698 (1996).
- [3] J.K. Fu, G. Atanassov, Y.S. Dai, F.H. Tan, Z.Q. Mo, *J. Non-Cryst. Solids* **218**, 403 (1997).
- [4] P. Park, S. Kang, *Appl. Phys. Lett.* **89**, 192905 (2006).
- [5] M. Ho, H. Gong, G. Wilk, B. Busch, M. Green, P. Voyles, D. Muller, *J. Appl. Phys.* **93**, 1477 (2003).
- [6] J. Wang, H. Li, R. Stevens, *J. Mater. Sci.* **27**, 5397 (1992).
- [7] J. Robbertson, *Rep. Prog. Phys.* **69**, 327 (2006).
- [8] D. M. Hausmann, R. G. Gordon, *Journal of crystal growth* **249**, 251 (2003).
- [9] M. Balog, M. Schieber, M. Michman, S. Patai, *Thin Solid Films* **41**, 247 (1977).
- [10] J. Lehan, Y. Mao, B.G. Bovard, H.A. Macleod, *Thin Solid Films* **203**, 227 (1991).
- [11] M. Zukic, D.G. Torr, J.F. Spann, M.R. Torr, *Appl. Opt.* **29**, 4284 (1990).
- [12] S.M. Edlou, A. Smajkiewicz, G.A. Al-Jumaily, *Appl. Opt.* **32**, 5601 (1993).
- [13] M. J. Madu, "Fundamentals of Microfabrication: The Science of Miniaturization", 2nd edn. CRCPress, Boca Raton, FL (2002).
- [14] R. K Nahar and Vikram Singh, *Microelectron. Internat.* **27**, 93 (2010).
- [15] R. Thielsch, A. Gatto, J. Heber, and N. Kaiser, in *Inorganic Optical Materials II*, A. J. Marker III and E. G. Arthurs, eds., *Proc. SPIE* **4102**, 276 (2000).
- [16] R. Chow, S. Falabella, G.E. Loomis, F. Rainer, C.J. Stolz, M.R. Kozlowski, *Appl. Opt.* **32**, 5566 (1993).
- [17] D. Reicher, P. Black, K. Jungling, *Appl. Opt.* **39**, 1589 (2000).
- [18] M. Ritala, M. Leskela, L. Niinisto, T. Prohaska, G. Friedbacher, M. Grasserbauer, *Thin Solid Films* **250**, 72 (1994).
- [19] J. Zhu, Z. G. Lie, Y. Feng, *J. Phys. D: Appl Phys.* **36**, 3051 (2003).
- [20] T. Tan, Z. Liu, H. Lu, W. Liu, H. Tian, *Opt. Mater.* **32**, 432 (2010).
- [21] J. Ni, Z.-C. Li, Z.-J. Zhang, *Front. Mater.Sci. China* **2**, 381 (2008).
- [22] M.F. Al-Kuhaili, S.M.A. Durrani, E.E. Khawaja, *J. Phys. D: Appl. Phys.* **37**, 1254 (2004).
- [23] G. He, L.Q. Zhu, M. Liu, Q. Fang, L.D. Zhang, *Appl. Surf.Sci.* **253**, 3413 (2007).
- [24] P.S. Lysaght, B. Foran, G. Bersuker, P.L. Chen, R.W. Murto, H.R. Huff, *Appl. Phys. Lett.* **82**, 1266 (2003).
- [25] J. Leger, A. Atouf, P. Tomaszewski, A. Pereira, *Phys. Rev. B* **48**, 93 (1993).
- [26] A.M. Al-Shukri, *Desalination* **209**, 290 (2007).
- [27] JCPDS database, International Center for Powder Diffraction Data, PA (1999).
- [28] B.D. Cullity, *Elements of X-ray Diffraction*, first ed., Addison-Wesley, (1977), p. 81
- [29] Y. Zhou, J. A. Switzer, *J. Alloys Compd.* **237**, 1 (1996).
- [30] M.F. Al- Kuhaili, *Opt. Mater.* **27**, 383 (2004).
- [31] L. Wang, B. Fan, Z. Wang, X. Cheng, Y. Wu, L. Chen, *Mater. Sci.-Poland* **27**, 547 (2009).
- [32] A.E. Owen, *Phil. Mag.* **27**, 1151 (1971).
- [33] N.F. Mott, E.A. Davis, *Electronic Processes in Non-Crystalline Materials*, second edn., Clarendon Press, Oxford, 1979.
- [34] J.I. Pankove, *Optical Processes in Semiconductors*, Dover, New York, 1975.
- [35] Y. Wang, Z. Lin, X. Cheng, H. Xiao, F. Zhang, S. Zou, *Appl. Surf. Sci.* **228**, 93 (2004).
- [36] A.F. Khan, M. Mehmood, A.M. Rana, M.T. Bhatti, A. Mahmood, *Chin. Phys. Lett.* **26**, 077803 (2009).
- [37] F. Urbach, *Phys. Rev.* **92**, 1324 (1953).
- [38] M.F. Wasiq, M.Y. Nadeem, F. Chollet, S. Atiq, *Key Eng. Mater.* **442**, 96 (2010).
- [39] M.H. Brodsky, "Amorphous Semiconductors", Springer, Berlin, (1979).
- [40] S. Zainobidinov, R.G. Ikramov, M.A. Nuritdinova, R.M. Zhalalov, *Ukr. J. Phys.* **53**, 1177 (2008).
- [41] M.C. Lovell, A.J. Avery, M.W. Vernon, "Physical Properties of Materials", ELDS Publishers, UK, (1984).
- [42] G.P. Smestad, "Optoelectronics of Solar Cells", SPIE Press, Washington, (2005), pp.27.
- [43] J. Wang, R.L. Maier, H. Schreiber, *Appl. Opt.* **47**, C189 (2008).

[44] M. Fadel, O.A. Azim M, O.A. Omer, R.R. Basily, *Appl. Phys. A: Mater. Sci. Process* **66**, 335 (1998).

[45] I. Fanderlik, "Optical Properties of Glasses", Elsevier, New York, (1983), p. 29.